Heliyon 10 (2024) e27170

Contents lists available at ScienceDirect

Heliyon

journal homepage: www.cell.com/heliyon

Research article

Identification of macrophage-related genes correlated with prognosis and immunotherapy efficacy in non-small cell lung cancer

Shaodi Wen [1], Renrui Zou [1], Xiaoyue Du, Rongtian Pan, Rutao Li, Jingwei Xia, Cong Xu, Ruotong Wang, Feng Jiang, Guoren Zhou, Jifeng Feng, Miaolin Zhu, Xin Wang [**], Bo Shen [*]

Department of Oncology, The Affiliated Cancer Hospital of Nanjing Medical University & Jiangsu Cancer Hospital & Jiangsu Institute of Cancer Research, Jiangsu, Nanjing 21000, China

ARTICLE INFO

Keywords:
Macrophage
Non-small cell lung cancer
Single cell RNA-seq
Bulk RNA-seq
Immune microenvironment

ABSTRACT

Background: Malignant tumours, particularly non-small cell lung cancer (NSCLC), pose a significant threat to human health due to their prevalence and lethality. Treatment methods for NSCLC vary greatly among individuals, making it crucial to identify predictive markers. Moreover, during tumour initiation and progression, tumour cells can release signaling molecules to induce polarization of macrophages towards a more tumour friendly M2 phenotype, which can promote tumour growth, metastasis, and drug resistance.

Methods: We employed a comprehensive approach, combining bulk RNA-seq and single-cell sequencing analysis.

Results: In our study, we used bulk RNA-seq and single-cell sequencing methods to analyze differential cells in NSCLC and adjacent tissues, searching for relevant marker genes that can predict prognosis and drug efficacy. We scrutinized biological phenomena such as macrophage-related gene methylation, copy number variation, and alternative splicing. Additionally, we utilized a co-culture technique of immune and tumour cells to explore the role of these genes in macrophage polarization. Our findings revealed distinct differences in macrophages between cancerous and adjacent tissues. We identified ANP32A, CCL20, ERAP2, MYD88, TMEM126B, TUBB6, and ZNF655 as macrophage-related genes that correlate with NSCLC patient prognosis and immunotherapy efficacy. Notably, ERAP2, TUBB6, CCL20, and TMEM126B can induce macrophage M0 to M2 polarization, promoting tumour proliferation.

Abbreviations: NSCLC, Non-small cell lung cancer; TAMs, Tumour-associated macrophages; scRNA-seq, Single-cell RNA sequencing; The Cancer Genome Atlas, TCGA; The Gene Expression Omnibus, GEO; The differentially expressed genes, DEG; Principal component analysis, PCA; Gene Set Enrichment Analysis, GSEA; T-distributed Stochastic Neighbor Embedding, t-SNE; gene ontology, GO; Kyoto Encyclopedia of Genes and Genomes, KEGG; Gene Set Variation Analysis, GSVA; eXtreme Gradient Boosting, XGBoost; the Area Under Curve, AUC; polymerase chain reaction, PCR; Copy number variation, CNV; Alternative splicing, AS; Percent spliced in, PSI.

* Corresponding author. Department of Oncology, The Affiliated Cancer Hospital of Nanjing Medical University & Jiangsu Cancer Hospital & Jiangsu Institute of Cancer Research, Jiangsu, Nanjing 21000, China.

** Corresponding author. Department of Oncology, The Affiliated Cancer Hospital of Nanjing Medical University & Jiangsu Cancer Hospital & Jiangsu Institute of Cancer Research, Jiangsu, Nanjing 21000, China.

E-mail addresses: wangxin00320@hotmail.com (X. Wang), shenbo987@njmu.edu.cn (B. Shen).

[1] Shaodi Wen and Renrui Zou contributed equally to this work.

https://doi.org/10.1016/j.heliyon.2024.e27170
Received 1 August 2023; Received in revised form 22 February 2024; Accepted 26 February 2024
Available online 7 March 2024

Conclusion: These findings significantly contribute to our understanding of the NSCLC tumour immune microenvironment. They pave the way for further research into the potential of these genes as targets for regulating tumour occurrence and development.

1. Introduction

Cancer remains one of the most significant health challenges facing humanity, and the COVID-19 pandemic has further complicated the diagnosis and treatment of certain cancers, leading to an increase in advanced cases. Lung cancer, in particular, is the second most prevalent cancer in both genders, with the highest mortality rate [1,2]. The disease predominantly affects the elderly, with a median age at diagnosis of over 65 years. Furthermore, the disease has a low overall 5-year relative survival rate, and many patients have pre-existing impaired lung function that can be worsened by treatment [3,4]. Unfortunately, the majority of lung cancer cases are diagnosed at an advanced stage, with only a small percentage identified at stage I. Patients diagnosed at this stage exhibit a 5-year survival rate of 65%, starkly contrasting with a mere 5% at stage IV [5]. Therefore, early detection of lung cancer patients is critical for improving survival rates. While chemotherapy, targeted therapy, and immunotherapy have shown promise in treating lung cancer, adverse drug reactions remain a common concern [6]. Moreover, not all patients benefit from these treatments, underscoring the need for effective biomarkers in lung cancer research.

In recent years, the field of tumour genomics has rapidly evolved, offering a myriad of sequencing techniques for analysing tissue genes, including whole-exome sequencing [7], transcriptome sequencing [8], chromatin immunoprecipitation sequencing [9], and single-cell sequencing [10]. Among these techniques, bulk RNA-seq has emerged as a popular choice due to its manageable cost, extensive public data availability, and its capacity to provide therapeutic and prognostic information. However, a key limitation of bulk RNA-seq is its inability to identify the gene expression characteristics of individual cells – the basic units of human structure and function - thereby limiting its usefulness in comprehensive research [7].On the other hand, Single-cell sequencing technology enables unbiased high-throughput analysis with minimal sample starting volume, and it can probe the functional state of individual cells [11,12]. It can also infer and discover new cell types in an unbiased manner and has greater sensitivity in quantifying rare variants and transcripts [10]. Despite its advantages, single-cell sequencing is costly, and the number of cells available for analysis is often limited compared to bulk RNA-seq sequencing. Furthermore, acquiring ample volumes of data on drug use and survival for analysis presents a challenge.

Tumour development and progression are complex processes involving a diverse array of cell types within the tumour microenvironment [13–15]. In particular, the tumour immune microenvironment has been shown to play a critical role in influencing the behaviour of malignant cells, including their response to therapy and overall prognosis [16,17]. Tumour-associated macrophages (TAMs), a major component of the tumour microenvironment, have been demonstrated to significantly impact disease progression in various cancers, including NSCLC [18,19]. TAMs are often characterized by an M2-like phenotype, which is associated with poor prognosis and resistance to therapy [20]. In fact, M2 macrophages are considered the most common type of TAM in the NSCLC microenvironment [21,22]. Identifying factors that induce M2 polarization is crucial for understanding the tumour immune microenvironment and for the development of effective therapeutic strategies. In this regard, numerous studies have concentrated on the role of macrophages in tumour development and progression, including their influence on the cycle of proliferation and apoptosis [23,24]. Furthermore, recent advances in single-cell sequencing technology have empowered researchers to scrutinize the tumour microenvironment with unprecedented resolution, facilitating the identification of new cell types and gene expression signatures potentially associated with disease progression and therapeutic response [25].

Our understanding of TAMs has matured over the past decades as we continues to unravel their complexities. Initially, TAMs were seen as immune system entities with the capability to target and engulf cancer cells, thus exhibiting antitumor functions [26]. However, further investigation into the biological complexities underlying tumour growth and metastasis has revealed that the tumour microenvironment can convert TAMs, or a subset thereof, into pro-cancer agents, thereby facilitating tumor progression [27]. An increased abundance of TAMs correlates with a general decline in patient survival across various cancer types [28]. The diversity of TAMs accounts for their multifaceted functions, as well as the presence of TAMs with potential antitumor capabilities [29]. As a result, it has become crucial to pinpoint markers that differentiate pro-tumor TAMs from anti-tumour TAMs. Conventional methods like flow cytometry and histology rely on a limited set of markers to characterize TAMs, and may not fully capture the extent of these cells' diversity or distinguish them from certain other cell populations. In recent years, single-cell omics methodologies have revealed the diversity of TAMs and reduced bias.

In summary, the intricate and dynamic tumour immune microenvironment plays a pivotal role in the initiation and progression of tumours. The skewed polarization of TAMs towards the M2 phenotype has been associated with unfavorable prognosis and therapy resistance in NSCLC. Therefore, the identification of factors promoting M2 polarization holds immense promise for improving NSCLC patient outcomes. Towards this end, we propose a method that combines bulk RNA-seq sequencing data with single-cell sequencing technology. This integrated approach will enable us to identify differentially expressed genes and immune cell types, pinpoint the most significant immune cells in the tumour microenvironment, unravel the key genes associated with them, and validate the findings with other datasets. Additionally, we will leverage functional and phenotypic experiments to unravel the upstream and downstream regulation of the identified genes. By doing so, we aim to pave the way for a deeper understanding of the tumour immune microenvironment in NSCLC and the identification of promising therapeutic targets for more effective treatments.

2. Methods

2.1. Datasets acquisition

To investigate the role of cell composition in NSCLC, we utilized a comprehensive approach combining bulk RNA-seq and single-cell sequencing analysis. We obtained bulk RNA-seq data for 454 NSCLC patients and normal tissues from The Cancer Genome Atlas (TCGA) database (https://portal.gdc.cancer.gov/). Out of these, we selected 337 patients with clinical information for survival analysis. To further explore the differences in cell composition between tumour and normal tissues, we used 10X single-cell sequencing data (GSE131907) obtained from the Gene Expression Omnibus (GEO) database (https://www.ncbi.nlm.nih.gov/geo). For validation of our findings, we also downloaded bulk RNA-seq data (GSE29013) from NSCLC patients with clinical information from the same database to serve as an external validation set.

2.2. Bulk RNA-seq data processing

To identify the differentially expressed genes (DEGs) in NSCLC, we employed a rigorous data analysis pipeline incorporating a combination of statistical methods and computational tools. Specifically, we obtained the TCGA dataset and classified the NSCLC data into tumours and paired normal tissues. We utilized the 'Deseq2' R package to perform differential expression analysis, identifying DEGs between the two groups. Principal component analysis (PCA) was then conducted to further investigate the differences in gene expression patterns. To visualize the results, we generated volcano plots highlighting the up- and down-regulated genes, labeling those exhibiting a |log FC| greater than 4-fold for further analysis. Additionally, we employed Gene Set Enrichment Analysis (GSEA) to identify differential gene enrichment pathways, providing insights into the biological processes and molecular mechanisms underlying NSCLC.

Furthermore, we selected 337 samples with survival data from the TCGA dataset and analysed the immune microenvironment of the tumour tissue using the 'xCell' R package. This comprehensive approach enabled us to obtain results for 61 immune cells and three immune infiltration scores. Subsequently, we analysed the relationship between immune cells and prognosis using the 'survminer' R package. We plotted survival curves using the Kaplan-Meier method, and employed log-rank tests to determine statistical significance, considering $P < 0.05$ as statistically significant. The integration of survival analysis with immune cell profiling allowed us to identify potential prognostic markers and therapeutic targets for NSCLC. Overall, our approach provides a powerful tool for the comprehensive analysis of NSCLC, and holds the potential to yield fresh insights into the molecular mechanisms and immunological features of this devastating disease.

2.3. Single-cell sequencing data processing

To obtain a comprehensive understanding of the cell composition differences between tumour and normal tissues in NSCLC, we utilized the 'Seurat' R package to analyze the 10X single-cell sequencing data (GSE131907). Specifically, we selected tumour and normal tissues numbered 06, 09, 20, 30, and 34 from the dataset for download, and performed a series of quality control checks to ensure the reliability and accuracy of our data analysis.

To this end, we examined the distribution of RNA feature numbers, absolute UMI counts, and mitochondrial genes for each sample, identifying samples with nFeature $\geq$2000, 2000 $\leq$ nCount $\leq$5000, and percent.mt $\geq$ 5%. These samples were subsequently used for downstream analysis. The data were then normalized and analysed using PCA to identify the major sources of variation in our dataset.

Next, we applied a downsampling strategy to ensure equal representation of all genes in our dataset, and automatically classified them into 40 clusters based on their expression patterns. To further refine our analysis, we used the fragmentation plot results to determine the PC values used for cell clustering. We then applied the T-distributed Stochastic Neighbor Embedding (t-SNE) algorithm to visualize the relationships between cells and calculated the maker genes for each cluster. Finally, we defined the clusters using the 'SingleR' R package, which allowed us to identify the cell types present in our dataset and compare their distribution between tumour and normal tissues.

2.4. Functional enrichment analysis

To gain insights into the biological functions and signaling pathways associated with the differentially expressed genes (DEGs), we conducted gene ontology (GO) pathway enrichment analysis, Kyoto Encyclopedia of Genes and Genomes (KEGG) pathway analysis, and Gene Set Variation Analysis (GSVA) using the 'clusterProfiler' package in R. The 'org.Hs.eg.db' package was used to annotate the genes, and the enriched pathways were visualized using 'plot' and 'ggplot 2' packages [30]. These analyses allowed us to identify the biological processes, molecular functions, cellular components, and signaling pathways significantly enriched in the NSCLC tumours.

2.5. Identification and screening of macrophage-related genes

To identify macrophage-related genes independently associated with prognostic outcomes in NSCLC, we extracted gene lists specifically expressed in macrophage clusters from single-cell RNA sequencing data. To pinpoint genes with independent prognostic significance, we utilized multiple machine learning algorithms, including Random Forest, eXtreme Gradient Boosting (XGBoost), and Lasso regression, in addition to traditional univariate and multifactorial Cox regression analyses. We evaluated the predictive power of

the model using the Area Under Curve (AUC) metric.

2.6. Drug efficacy and survival outcomes analysis

To investigate the potential role of macrophage-related genes in predicting the efficacy of immunotherapy in NSCLC, we used an online tool (http://rocplot.org/) to evaluate their predictive power. Furthermore, we assessed the relationship between these genes and survival outcomes using Kaplan-Meier curves and log-rank tests. The results of these analyses provide important insights into the potential utility of macrophage-related genes as biomarkers for predicting response to immunotherapy in NSCLC patients.

2.7. Cell experiments

Human myeloid leukemia mononuclear cells (THP-1 cells) were used as a cellular model to induce differentiation into macrophages. They were exposed to 185 ng/ml phorbol 12-myristate 13-acetate (PMA, S1819 Beyotime) in dimethyl sulfoxide (DMSO) for 6 h, which led to the acquisition of M0 cells. Next, the target gene, which can modulate macrophage polarization from the M0 to M2 phenotype, was used as the experimental group with siRNA interference in H23 cells, while H23 cells transfected with negative control siRNA served as the control group. The resulting macrophages were co-cultured with H23 cells to promote M2 polarization. The levels of ARG1 and FIZZ1, which are M2 polarization markers, were detected using polymerase chain reaction (PCR) technology.

Based on the PCR results, we identified genes potentially impacting macrophage polarization and aimed to confirm their role in lung cancer cells. To do this, we performed siRNA interference and CCK8 assays on H23 cells with low expression of the identified genes. Please refer to Supplementary tables 7 and 8 for the gene sequences involved in the siRNA interference experiment and the primer sequences used in the PCR experiment, respectively.

2.8. Methylation & copy number variation

To explore the relationship between the expression and methylation of the identified macrophage-related genes, we utilized the mutation module in the Gene Set Cancer Analysis online database (http://bioinfo.life.hust.edu.cn/web/GSCALite/). This allowed us to analyze the differences in methylation and copy number variation (CNV) of the genes between tumour and normal tissues. By integrating the data on expression, methylation, and CNV data, we aimed to gain a more comprehensive understanding of the molecular mechanisms of macrophage-related genes in lung cancer.

2.9. Alternative splicing & protein structure prediction

In this study, we aimed to investigate the potential clinical relevance of alternative splicing (AS) events in macrophage-related genes. To this end, we utilized the ClinicalAS module of the OncoSplicing server (http://www.OncoSplicing.com/) to identify AS events in these genes from the SplAdder and SpliceSeq projects. We further compared the percent spliced in (PSI) differences in AS events between tumour and normal using PanDiff plots. To explore the prognostic significance of AS events in cancer, we plotted Kaplan-Meier curves. Additionally, we predicted the protein structures of the AS isoforms using the structure module of the Human Protein Atlas Database.

2.10. Statistical analysis

In this study, all statistical analyses were conducted using the widely used R software (version 4.1.2). Survival analyses were performed using the 'survminer' R package in R. To determine the best cut-off values, the surv_cutpoint function was utilized. The risk score for the model was calculated by multiplying the expression of each gene by its corresponding regression coefficient and then adding them, as follows: risk score = expression of gene 1 $\times$ β1gene1 + expression of gene 2 $\times$ β2gene2 + ... + expression of genen $\times$ βngenen. A P-value less than 0.05 was considered statistically significant.

The normality and homogeneity of the PCR data and M2 polarization marker data were assessed using the Shapiro-Wilk test and the Levene's test, respectively. A P-value greater than 0.05 indicated that the data were normally distributed with equal variance. Parametric tests were employed if the data met these criteria. For comparing multiple datasets, analysis of variance (ANOVA) was utilized, whereas the *t*-test was employed for comparing two datasets.

3. Results

3.1. Study design

In this study, we conducted a comprehensive analysis of the differences between tumour and normal tissues of NSCLC patients using RNA-seq data from the TCGA database. Using bioinformatic analysis, we performed a survival analysis of immune infiltration-related cells to identify potential prognostic biomarkers. We then downloaded NSCLC single-cell sequencing data from the GEO database and analysed the differentially expressed cells, selecting tumours and normal tissues from five groups of NSCLC patients. The clinical information of the patients is detailed in Supplementary table 1.

Combining the findings from bulk RNA-seq and single-cell sequencing, we identified macrophages as differentially expressed in

tumour and normal tissues. We performed enrichment analysis of macrophage-related genes and developed a predictive model using machine learning and other methods. We validated the prediction model using the GSE29013 dataset and evaluated the predictive power of macrophage-related genes as potential drug targets using an online database.

To further investigate the function of these genes in NSCLC patients, we conducted several mechanistic studies and in vitro experiments. The overall flow of the study is presented in Fig. 1.

3.2. Tumour microenvironment analysis in NSCLC patients by combined bulk RNA-seq and scRNA

In this study, we conducted a comprehensive analysis of RNA-seq data from NSCLC patients in the TCGA and GEO databases to investigate the differences between tumour tissues and normal tissues. Principal component analysis (PCA) was performed using tumour and normal tissues from NSCLC patients in TCGA, reveling a clear distinction between tumour samples and normal samples (Fig. 2A). Differential analysis based on $|\log FC| \geq 1.5$ and FDR <0.05, was then performed on the sequencing results of tumour and normal tissues, with genes exhbiting $|\log FC| \geq 4$ being labeled (Fig. 2B). Gene set enrichment analysis (GSEA) revealed that the genes differentially expressed between tumour and normal tissues in the bulk RNA-seq analysis were mainly clustered in hallmark myc targets V2 and V1, hallmark E2F targets, and hallmark G2M checkpoint (Fig. 2C and D).

Furthermore, we analysed the immune infiltrating cells in the tumour microenvironment of NSCLC patients using the 'xCell' R package. We identified twenty-eight of the sixty-one immune cells that were associated with patient outcomes (supplementary figure

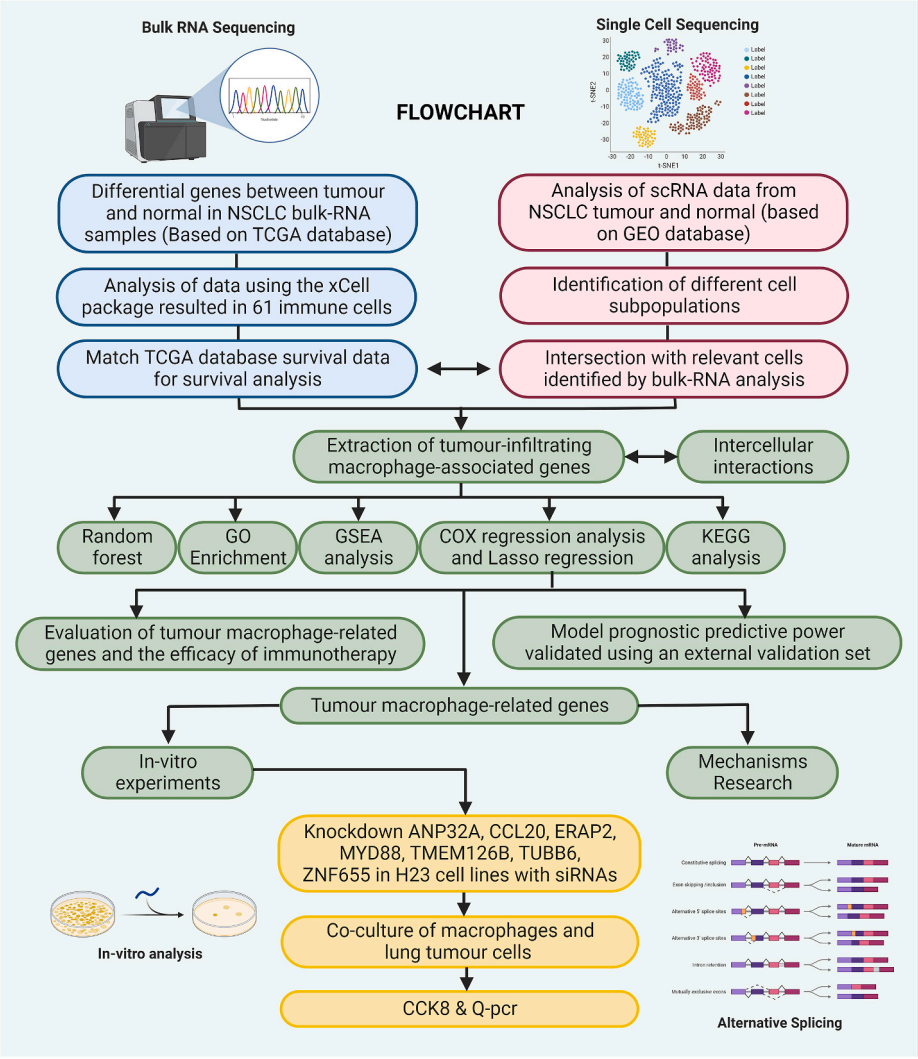

Fig. 1. Flowchart illustrating the study's methodology. The blue section represents the analysis of bulk RNA-seq data, while the red section depicts scRNA analysis. The green section shows the joint analysis, and the yellow section represents the in vitro experiments. This schematic was created using BioRender.com. (For interpretation of the references to color in this figure legend, the reader is referred to the Web version of this article.)

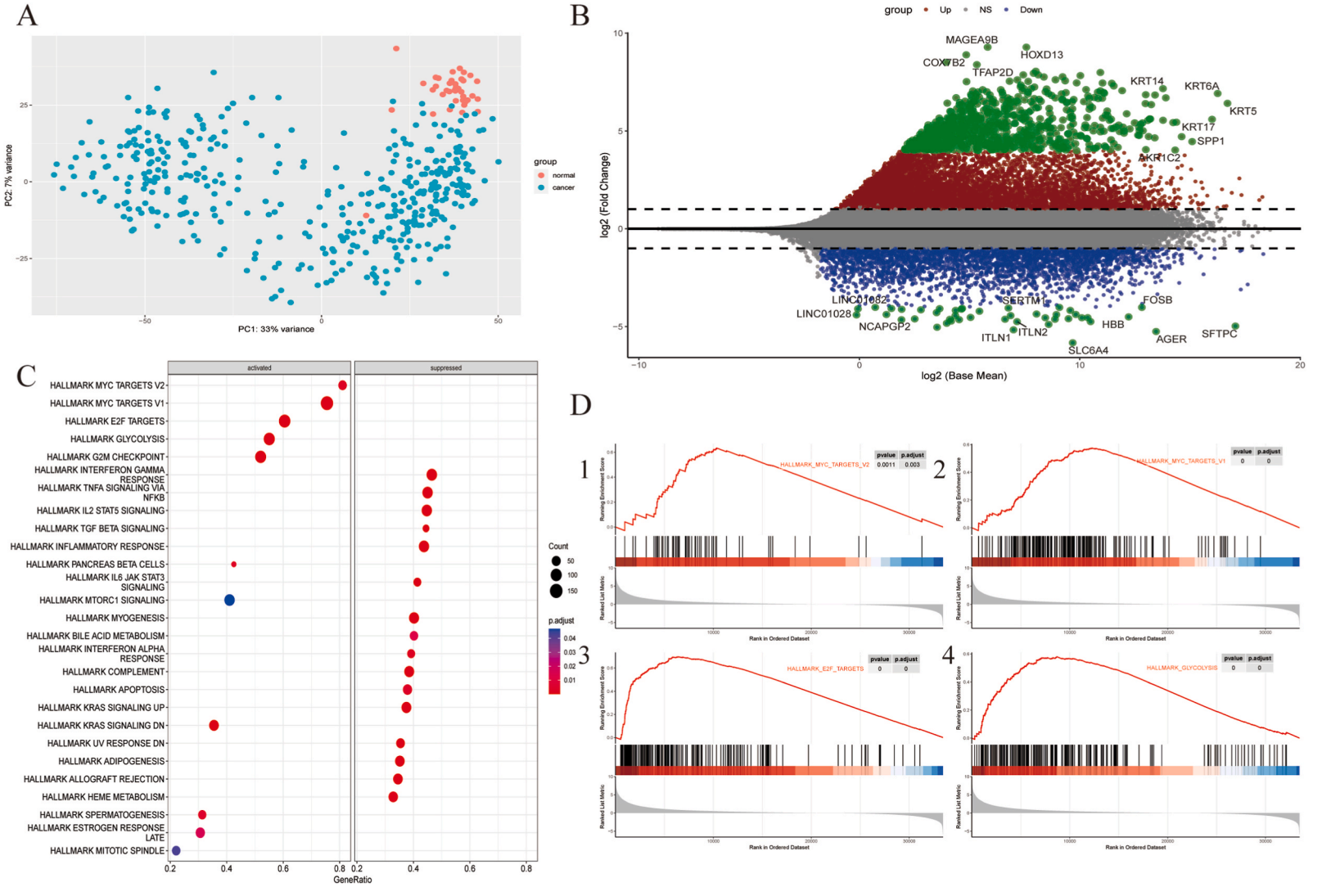

Fig. 2. TCGA's bulk RNA-seq data analysis. A. Principal component analysis (PCA) was performed using tumor and normal tissues from NSCLC patients. B. Volcano plot of differential genes, and genes with $|\log FC| \geq 4$ were labeled. C. Gene set enrichment analysis (GSEA) in hallmark. D. GSEA results for hallmark myc targets V2 and V1, hallmark E2F targets, and hallmark G2M checkpoint.

1), and the p-values for the relationship between immune cells and survival were also presented (supplementary table 2).

To gain further insights into the differential gene expression in tumour and normal tissues, we analysed scRNA data from the GSE131907 dataset. After quality control, we identified 40 clusters of cells based on the gene expression profile (supplementary fig. 2C-E), and we obtained 18 clusters (Fig. 3A and B). We found that clusters 2, 3, 4, 7, and 12 were significant differences between tumour and normal tissues (Fig. 3C and D). After annotation using SingleR automated annotation, we re-annotated the genes (Fig. 3E and F and supplementary table 3). We also observed that the cell clusters varied between separate samples (Fig. 3G), and the proportion of other clusters varied from one sample to another(supplementary figure 3A).

Based on the bulk RNA-seq data analysis, we found that differential expression of B-cells and macrophages across various tissues. In particular, the expression of B cells was associated with a better prognosis of NSCLC patients (Fig. 3H). However, macrophages expression was more complex, exhibiting differences across various macrophage types (Fig. 3I–K).

Moreover, we extracted data on immune cells in scRNA and annotated these cells using different makers according to the CellMaker database (supplementary table 4). We found that immune cell interactions were more frequent in normal tissues compared to tumour tissues (Fig. 4A–C). In normal tissues, intercellular interactions (Fig. 4B) predominantly involved T cells with macrophages (INFG-INFGR1, INFGR2), macrophages with other macrophages (CCL23-CCR1), NK cells with macrophages (INFG-INFGR1, INFGR2), and mast cells with macrophages (LIF-IL6ST). In contrast, in tumour tissues (Fig. 4D), interactions were observed between macrophages and other macrophages (IL15-IL15RA, IL6-IL6R, CCL13-CCR1, CCL23-CCR1), as well as between macrophages and mDC cells (LNG-NOTCH2).

We performed differential gene analysis on the extracted macrophages to gain further insights into the molecular mechanisms underlying NSCLC. We analysed both up-regulated and down-regulated genes in macrophage-related genes (Fig. 4E), and conducted GO enrichment analysis (Fig. 4F). As shown in Fig. 4G–K, the GSEA analysis suggested that the differential genes were mainly clustered

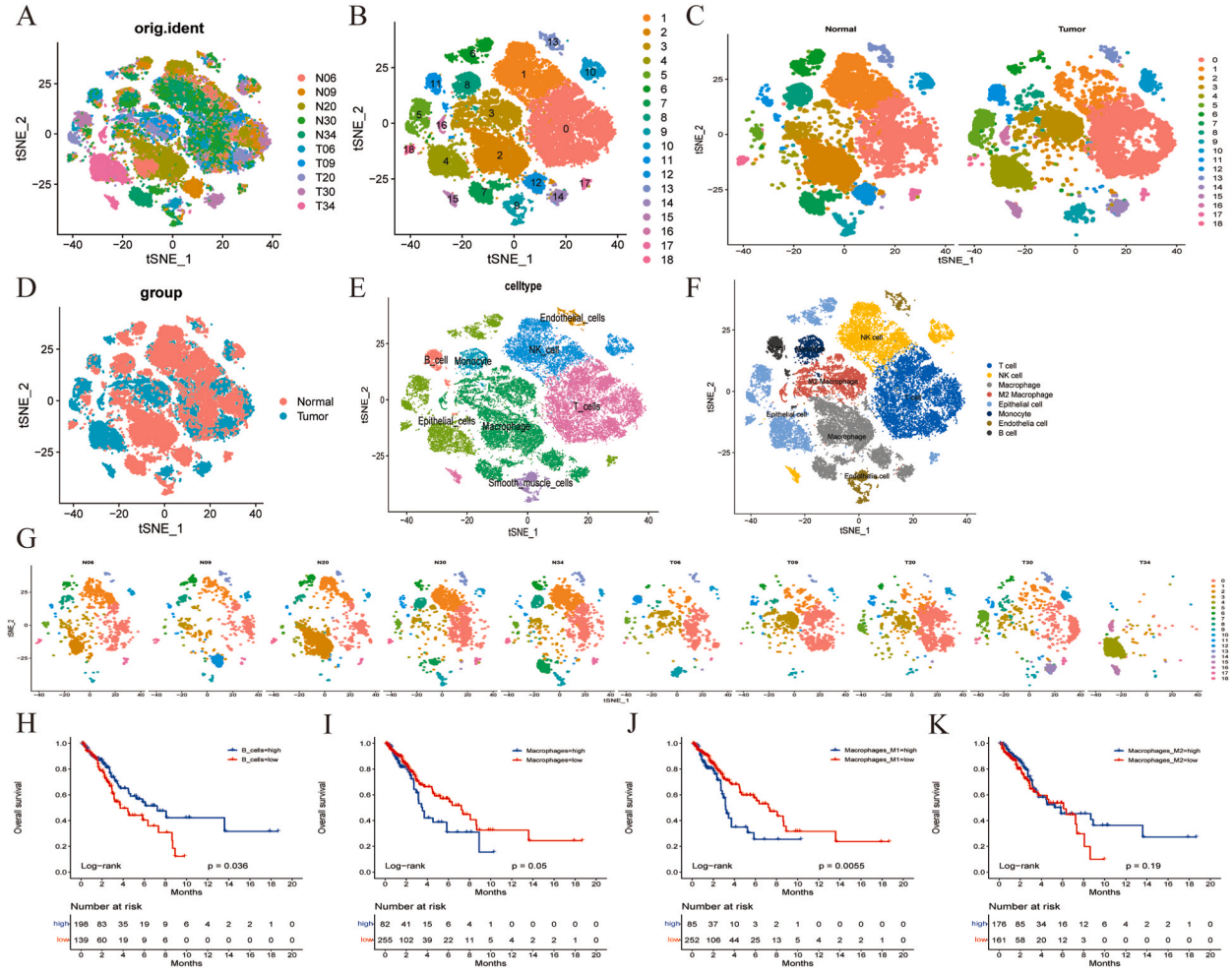

Fig. 3. Analysis of scRNA data. A. tSNE analysis of paired normal and tumour samples. B. Clustering of cells into 18 clusters. C and D. Distribution of clusters in normal and tumour tissues. E. tSNE map automatically annotated using SingleR. F. Renamed tSNE profiles. G. Composition of each sample's clusters. H–K. Kaplan-Meier curves of differential cells.

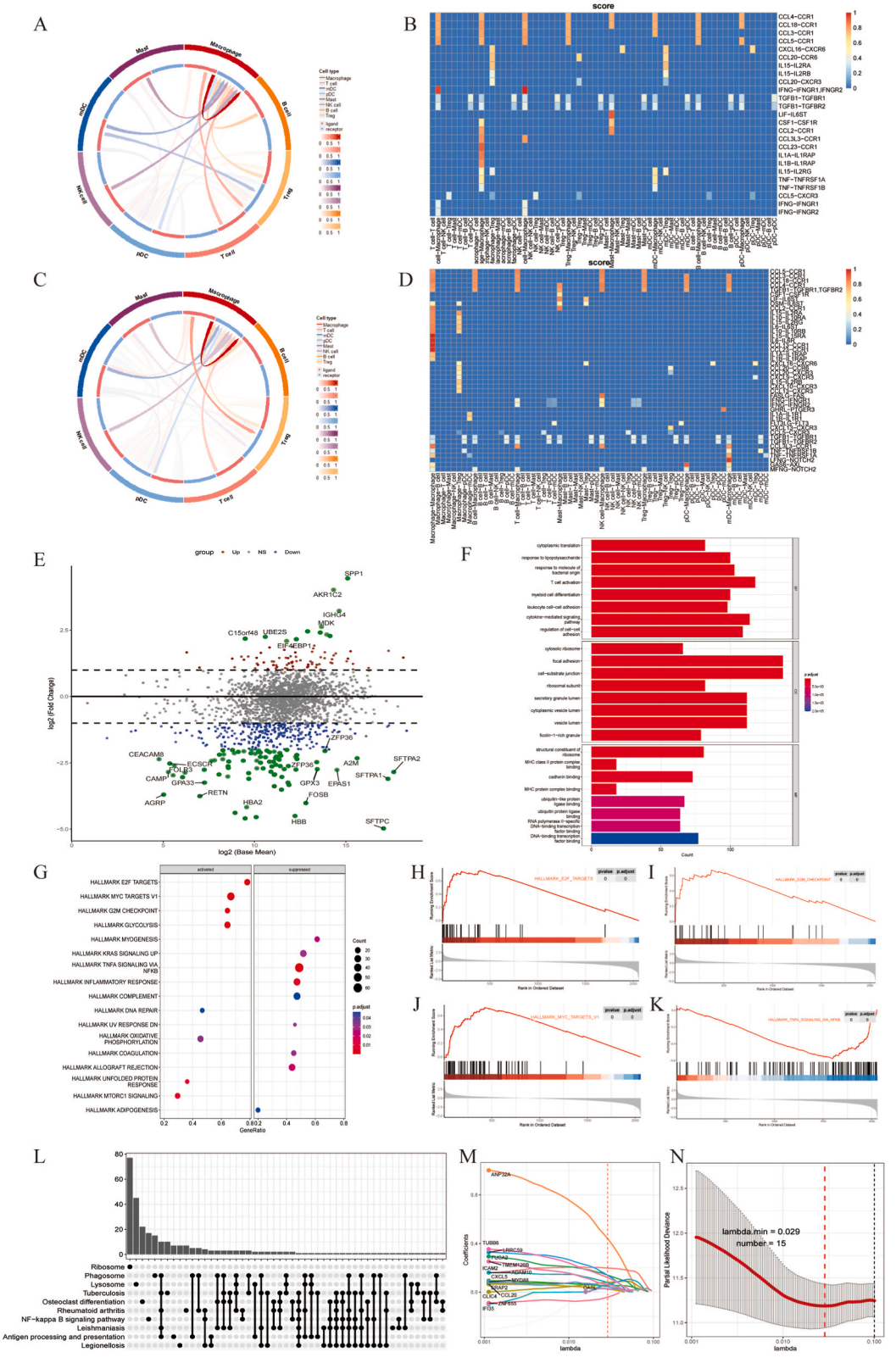

(caption on next page)

Fig. 4. Analysis of the tumour immune microenvironment in NSCLC based on scRNA analysis. A and B. Cell-cell interaction analysis in normal tissues. C and D. Cell-cell interaction analysis in tumour tissue. E. Volcano plot showing differentially expressed macrophage-related genes. F. Gene ontology (GO) enrichment analysis map for macrophage-related genes. G. Gene set enrichment analysis (GSEA) results for macrophage-related genes. H–K. GSEA analysis for hallmark E2F targets, hallmark myc targets V1, hallmark G2M checkpoint, and hallmark glycolysis. L. Kyoto Encyclopedia of Genes and Genomes (KEGG) analysis of macrophage-related genes. M and N. Lasso regression analysis of macrophage-related genes and prognosis.

in hallmark E2F targets, hallmark myc targets V1, hallmark G2M checkpoint, and hallmark glycolysis. Interestingly, these pathways did not align precisely with those identified in the bulk RNA-seq analysis, highlighting the importance of studying specific cell populations to gain a more comprehensive understanding of the disease. Furthermore, KEGG pathway analysis showed that macrophage-associated differential genes were primarily enriched in Ribosome, Phagosome, Lysosome, and Tuberculosis pathways (Fig. 4L), potentially reflecting the involvement of macrophages in diverse biological processes, such as protein synthesis, degradation, and immune defense. These findings illuminate the complex molecular mechanisms underlying NSCLC and may suggest new targets for therapeutic intervention.

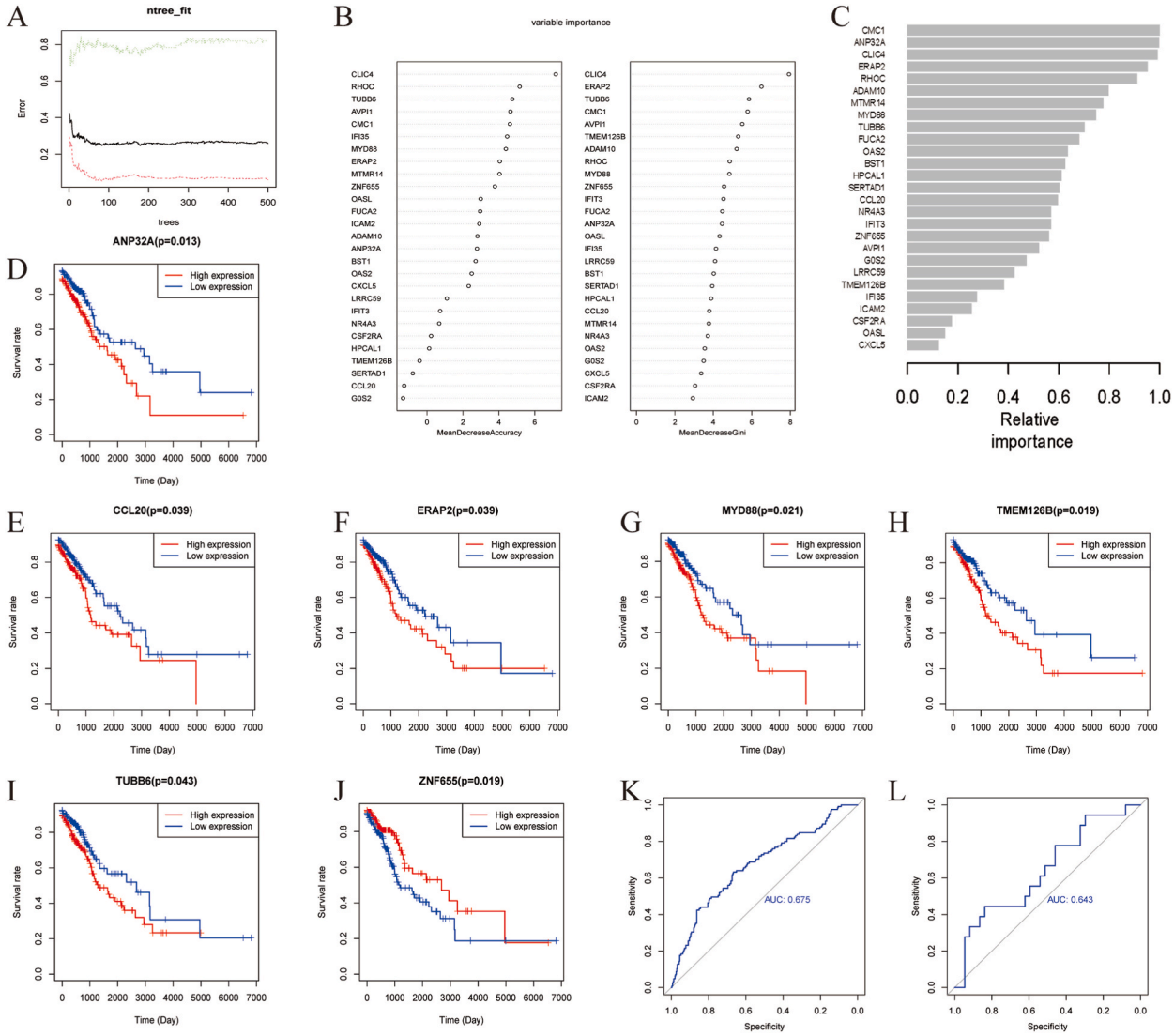

Fig. 5. Prognostic analysis of macrophage-related genes. A. Random Forest analysis of macrophage-related genes. B. Gene importance ranking based on Random Forest analysis. C. Gene importance ranking based on XGBoost analysis. D-J. Prognostic analysis of macrophage-related genes using machine learning and Cox regression analysis. K. ROC plot showing the prognostic predictive ability of the training set. L. ROC plot showing the predictive prognostic ability of the validation set.

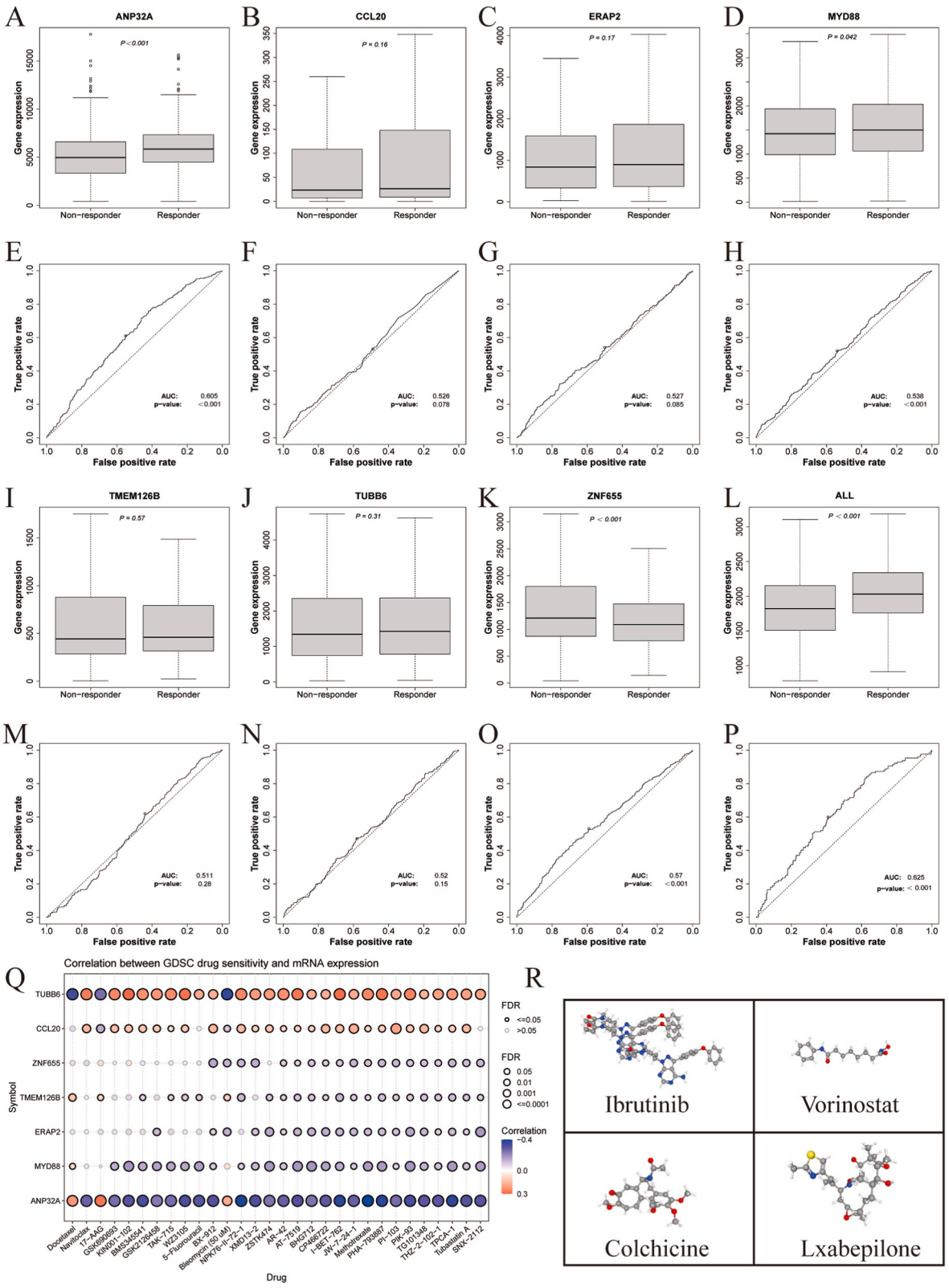

(caption on next page)

Fig. 6. Relationship between macrophage-related genes, treatments, and drugs in NSCLC. A-D. Differential expression of ANP32A, CCL20, ERAP2, and MYD88 between responders and non-responders to immunotherapy. E-H. ROC curves of ANP32A, CCL20, ERAP2, and MYD88 in predicting immunotherapy response. I-L. Differential expression of TMEM126B, TUBB6, ANF655, and models between responders and non-responders to immunotherapy. M-P. ROC curves of TMEM126B, TUBB6, ANF655, and models in predicting immunotherapy response. Q. Correlation analysis between macrophage-related gene expression and drug sensitivity using the Genomics of Cancer Drug Sensitivity (GDSC) database. R. Known gene-drug interactions in the Drug-Gene Interaction Database (DGIdb) (https://DGIdb.genome.wustl.edu/), with identified drugs and their 3D structures obtained from the PubChem website (https://pubchem.ncbi.nlm.nih.gov/).

3.3. Identification of macrophage-related genes and evaluation of their clinical values

The present study aimed to identify novel macrophage-related genes that could serve as independent predictors for the progression of NSCLC. To achieve this, we extracted macrophage-associated genes fromSupplementary table 5 and integrated predictive data from the TCGA dataset, applying lasso regression analysis to 101 genes (Fig. 4M). To ensure the robustness of our findings, we conducted ten-fold cross-validation to optimize parameter selection in the Lasso model. Our analysis revealed that lambda = 0.029 for 15 genes included in the model (Fig. 4N).

Next, we performed random forest (Fig. 5A and B) and xgboost analyses (Fig. 5C), ranking the genes according to their importance. We also conducted univariate Cox regression analysis and identified 27 genes associated with prognosis (supplementary table 6). By in tegrating the Lasso model, random forest, XGBoost, and multivariate Cox regression analysis, we identified seven macrophage-related genes - ANP32A, CCL20, ERAP2, MYD88, TMEM126B, TUBB6, and ZNF655 - as independent predictors of NSCLC progression.

Furthermore, we assessed the expression density of the seven macrophage-related genes and found that they were mainly distributed in the annotated macrophage cluster (supplementary fig. 3C - I). Detailed analysis revealed that CCL20, ERAP2, MYD88, and TUBB6 were primarily clustered within the macrophage compartment, while ANP32A, TMEM126B, and ZNF655 were enriched across multiple clusters (supplementary fig. 4A - N). These findings offer fresh insights into the role of macrophage-associated genes in NSCLC progression and may have significant implications for the development of novel therapeutic strategies.

3.4. The potential value of macrophage-related genes as indicators of drug efficacy

To evaluate the potential of macrophage-related genes in predicting immunotherapy outcomes in NSCLC patients, we employed a publicly available online tool (http://rocplot.org/) to assess the predictive power of individual genes. Our results revealed that ANP32A, MYD88, and ZNF655 were significantly associated with immunotherapy efficacy in NSCLC patients ($P < 0.05$, Fig. 6A–D, E, H, K, O). However, the remaining genes showed no predictive value for immunotherapy outcomes (Fig. 6B, C, F, G, I, J, M, N). Despite this, our developed predictive model exhibited some predictive power for immunotherapy in NSCLC patients (AUC = 0.625, $P < 0.05$, Fig. 6L–P), surpassing the predictive power of individual genes.

Moreover, we investigated the correlation between the expression of macrophage-related genes and drug sensitivity using the Genomics of Drug Sensitivity in Cancer (GDSC) database. Interestingly, we found that TUBB6 showed a positive correlation with the top 30 GDSC drugs, whereas ANP32A demonstrated a negative correlation with these drugs (Fig. 6Q). We also examined known drug interactions of the genes in the Drug Gene Interaction Database (DGIdb) (https://DGIdb.genome.wustl.edu/) and identified drugs that corresponded to prognosis. The 3D structures of these drugs were displayed using the PubChem website (https://pubchem.ncbi.nlm.nih.gov/) (Fig. 6R).

3.5. Co-culture of macrophages and lung tumour cells

To further investigate the impact of macrophage-related genes on macrophage polarization, we conducted siRNA interference experiments targeting ANP32A, CCL20, ERAP2, MYD88, TMEM126B, TUBB6, and ZNF655 genes in H23 cells (supplement table 7). We verified the knockdown efficiency by extracting cellular RNA and reverse-transcribing it into cDNA for PCR analysis (supplement figure 5). Subsequently, we co-cultured H23 cells and macrophages in the M0 state at a ratio of 1:8 for 72 h and extracted macrophage RNA to detect the levels of M2 polarization markers, ARG1 and FIZZ1, using PCR. Our results revealed that the knockdown of ERAP2, TUBB6, CCL20, and TMEM126B genes led to a decrease in the expression of the M2 polarization marker, ARG1, when compared to the control group (Fig. 7A). On the other hand, the knockdown of ZNF655 resulted in a significant increase in FIZZ1 expression compared to the control group. Conversely, the expression of FIZZ1 decreased to varying degrees after knocking down other macrophage-related genes (Fig. 7B). These findings suggest that knockdown of ZNF655 promotes the polarization of M0 to M2, whereas knockdown of the other six genes inhibits M0 to M2 polarization. Our preliminary analysis suggests that, except for the ZNF655 gene, which appears to be a tumour suppressor gene, the other six genes may function as tumour-promoting genes. Knockdown of these genes affects the polarization of M0 to M2, thus affecting the impact of macrophages on tumour cells.

3.6. Influence of macrophage-related genes on tumour cells

To explore the potential influence of macrophage-associated genes on lung cancer cells, we targeted genes implicated in M0 to M2 polarization, specifically ERAP2, TUBB6, CCL20, and TMEM126B, using siRNA interference. Besides assessing the levels of M2 polarization markers, we also evaluated the impact of gene knockdown on tumor cell proliferation. Our results showed that knockdown of these genes significantly inhibited tumour cell growth (Fig. 7C–F), with CCL20 and TMEM126B exhibiting the most pronounced

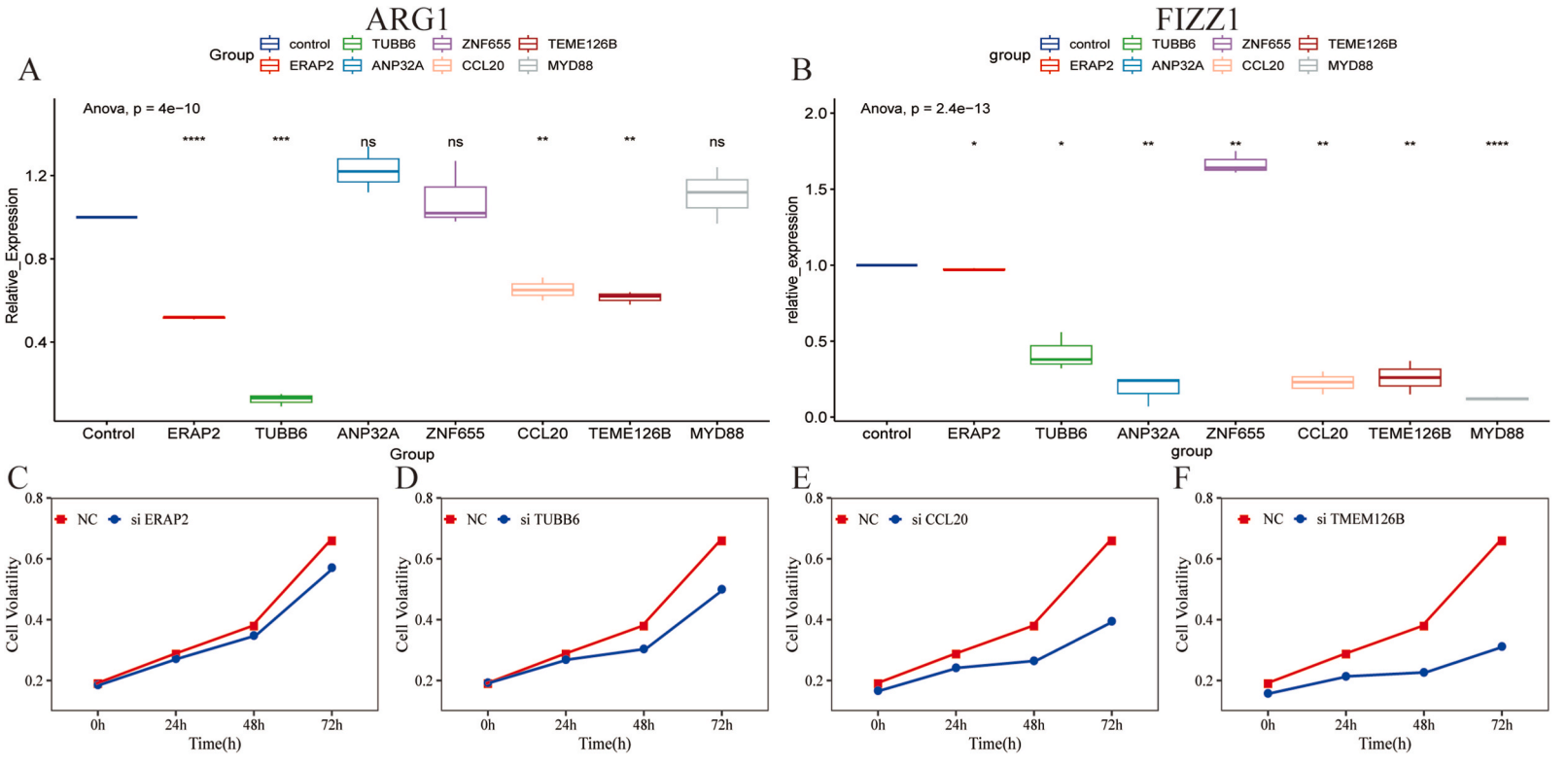

Fig. 7. Effects of macrophage-related genes on M2 polarization and NSCLC cells. A. Expression of ARG1 after knockouts of ERAP2, TUBB6, ANP32A, ZNF655, CCL20, TMEM126B and NYD88. B. Expression level of FIZZ1 after knockouts of ERAP2, TUBB6, ANP32A, ZNF655, CCL20, TMEM126B and NYD88. C–F. NSCLC cell volatility after knockouts of ERAP2, TUBB6, CCL20, and TMEM126B.

effects. These findings suggest that these genes may act as tumour suppressors by inhibiting the M0-to-M2 polarization, ultimately leading to reduced tumour cell proliferation.

3.7. Methylation and copy number variation of macrophage-related genes

In this part, we aimed to investigate the methylation status and copy number variations (CNVs) of macrophage-related genes in NSCLC patients. Our analysis indicated that TMEM126B did not show differential methylation between cancerous and normal tissues in lung adenocarcinoma, whereas ZNF655 data was missing for lung adenocarcinoma. However, other macrophage-related genes showed significant differences in methylation status in both cancer and normal tissues, as demonstrated in Supplementary fig. 6 A - L.

To further explore the relationship between methylation and mRNA expression of macrophage-related genes, we analysed the correlation between mRNA expression and methylation levels of these genes in both lung squamous carcinoma and lung adenocarcinoma. Interestingly, we discovered that the mRNA expression of ZNF655 was inversely correlated with its methylation in lung squamous carcinoma, whereas the mRNA expression of CCL20 was inversely correlated with its methylation in lung adenocarcinoma, as illustrated in Supplementary figure 6M.

In addition to analyzing methylation, we also investigated the CNVs of macrophage-related genes in NSCLC patients. Our findings indicated that the frequency of CNV amplification for ZNF655, TMEM126B, and TUBB6 was highest in lung cancer, as depicted in Supplementary figure 6 N. Moreover, we observed that differences in immune infiltration between CNV groups of macrophage-associated genes were elevated in macrophages, as shown in Supplementary figure 6 O.

Based on our findings, we suggest that the expression of macrophage-associated genes in macrophages may be affected by methylation or CNV. It is known that gene expression is negatively correlated with the degree of methylation, while the abundance of CNAs is positively correlated with gene expression. These findings provide valuable insights into the regulation of macrophage-associated genes in NSCLC and may have implications for the development of novel therapeutic strategies.

3.8. Alternative splicing and protein structure prediction of macrophage-related genes

In our investigation of macrophage-related genes, we uncovered intriguing insights into the impact of alternative splicing on the prognosis of lung cancer. Specifically, our analysis demonstrated that patients with increased alternative splicing of the ZNF655 gene exhibited a more favorable prognosis in lung cancer, whereas enhanced alternative splicing of other genes correl ated with a poorer prognosis (see Supplementary figures 7-8). Moreover, we observed differences in the alternative splicing of ERAP2 among different types of lung cancer.

Further analysis of the Percent Spliced In (PSI) differences between tumours, adjacent normal tissues, and tumour and GTEx normal tissues revealed significant variations in different macrophage-related genes among different types of tumours (Supplement fig. 9A-G). Notably, utilizing the Human Protein Atlas database enabled us to predict the protein structures of these macrophage-related genes (refer to Supplementary fig. 9H-N). Th ese findings suggest that alternative splicing may play a critical role in shaping the structures of the proteins encoded by these genes, which could have important implications for their function in the context of lung cancer.

4. Discussion

In this study, we performed a comprehensive analysis of tumour and normal tissues from NSCLC patients using RNA-seq data from the TCGA and GEO databases. We identified macrophages as being differentially expressed between tumour and normal tissues and found that macrophage expression was associated with the prognosis of NSCLC patients. Moreover, we developed a predictive model using machine learning and other methods, identifying seven macrophage-related genes as independent predictors of NSCLC progression. We also evaluated the potential of macrophage-related genes to predict immunotherapy outcomes and drug sensitivity. In addition, we conducted mechanistic studies and in vitro experiments to investigate the impact of macrophage-related genes on macrophage polarization and tumour cell proliferation. Finally, we analysed the methylation and copy number variation of macrophage-related genes in NSCLC patients. Lastly, we analysed the methylation status and copy number variations of macrophage-related genes in NSCLC patients.

The immune cells identified in bulk RNA-seq samples using the xCell R package differ from those identified at the single-cell RNA level, demonstrating differences in gene enrichment pathways. Of the seven genes identified through machine learning and Cox multivariate regression analysis, six have been implicated in cancer promotion, while ZNF655 functions as a tumour suppressor. Notably, ERAP2, TUBB6, CCL20, and TMEM126B play a critical role in M2 macrophage polarization (Fig. 7A and B).

ERAP2 (Endoplasmic Reticulum Aminopeptidase 2) is a member of the oxytocinase subfamily of M1 aminopeptidases and closely related to its homologous enzyme ERAP1 [31]. It plays a crucial role in cancer, infection, and autoimmune diseases. Multiple previous studies have shown that ERAP2 is upregulated in tumour patients, leading to higher survival rates [32–34]. However, the highly variable and independent expression of ERAP2 across all cancer cell lines, as revealed by a comparison of ERAP2 tissue distribution between human tumours and their corresponding normal tissues, may contribute to tumour immunoediting. Additionally, our study employed scRNA analysis, yielding results not entirely consistent with previous findings obtained using bulk RNA-seq [32]. ERAP2 is downregulated in response to all live bacteria or bacterial stimuli, showing a strong association with macrophages [35].

Tubulin plays a crucial role in tumorigenesis and has shown potential prognostic value in various solid tumours [36,37]. Recent studies have demonstrated that TUBB6 (tubulin beta 6 class V) promotes the growth of cancer tissue in multiple solid tumours and serves as an important prognostic factor [38–40]. Our findings further support this concept. However, our results indicate that

TUBB6's predictive role in immunotherapy efficacy is unsatisfactory (see Fig. 6J and N).

The crucial role of the CCL20-axis in the polarization of M2 macrophages has been extensively investigated [41,42]. CCL20, a chemokine known to be secreted by a variety of immune cells [43–45], has been found to be highly expressed in lung cancer recurrence [46]. Our study corroborates these findings and highlights that elevated levels of CCL20 are associated with poor prognosis and increased M2 polarization (see Figs. 5E and 7E). Our analysis also suggests that the CCL20-CCR6 axis may play a crucial role in these processes, as evidenced by its enrichment in our cell-cell interaction analysis of normal tissues (see Fig. 4B).

TMEM126B (Transmembrane protein 126B) serves as an assembly factor for complex I, and its deficiency is linked to reduced cellular respiration [47,48]. Chronic hypoxia induces TMEM126B degradation [49]. Despite its importance in mitochondrial function, TMEM126B's role in tumorigenesis has been largely unexplored, partly because its targeting may result in lethal damage or side effects. Nevertheless, its effect on M2 polarization cannot be ignored, especially considering its role in coordinating metabolic and pro-inflammatory cytokine production in classically activated macrophages through hypoxia-inducible factor (HIF)-1α. Recent studies have revealed that TMEM126B knockdown results in succinate accumulation, with a direct connection to HIF-1-mediated pro-inflammatory macrophage activation [50]. In summary, our understanding of TMEM126B's role in tumorigenesis remains incomplete and calls for further investigation.

We found that the degree of DNA methylation of ANP32A, CCL20, MYD88, and TMEM126B was reduced in NSCLC, while the degree of methylation of ZNF655 was increased (Figure S6A-L). Notably, the DNA methylation of TUBB6 showed opposite trends in LUAD and LUSC (Figure S6A-L). We also observed a negative correlation between DNA methylation and mRNA expression of these genes (Figure S6M). Furthermore, we performed additional analyses and found that the expression of these genes affects copy number variations (CNVs), resulting in the enrichment of immunosuppressive cells (Figure S6N-O).These findings suggest that DNA methylation regulates the expression of these genes in NSCLC and may affect the enrichment of immune cells through CNVs, leading to tumor immune escape and regulation by DNA methylation of immunity. Our study provides new insights into the mechanisms underlying the development and progression of NSCLC, and we plan to conduct further research in this area.

Although our study provides new insights into the characterization of macrophages and key genes in the tumour immune microenvironment of NSCLC, as well as proposing new markers for predicting the prognosis of NSCLC patients and the efficacy of immunotherapy, our study has several limitations. First, our data were obtained from publicly available online datasets, and we were unable to perform quality control on the tissue source of the sequencing data. Second, although we made efforts to remove the batch effect using bioinformatics methods, it may still exist. Third, research on the mechanism of macrophage-related genes remains limited. In future studies, we plan to address these limitations by collecting clinical samples for sequencing after strict quality control, and conducting in-depth research on genes that affect macrophage polarization. We anticipate that our findings will contribute to the development of more efficacious therapeutic strategies for NSCLC patients.

In summary, our study utilized joint analysis and in vitro cell co-culture methods to investigate the differentially expressed macrophages and related genes affecting M2 polarization in the NSCLC tumour immune microenvironment. Our findings reveal that ERAP2, TUBB6, CCL20, and TMEM126B play pivotal roles in the polarization of M2 macrophages, and significantly impact the prognosis of NSCLC and the efficacy of immunotherapy. These findings provide valuable insights into the underlying mechanisms of NSCLC and may have implications for the development of new therapeutic strategies.

5. Conclusions

By jointly applying single-cell sequencing and bulk RNA-seq methodologies for NSCLC data analysis, we highlighted the crucial role that macrophages play in NSCLC. Notably, the ERAP2, TUBB6, CCL20, and TMEM126B genes emerged as key regulators of M2 cell polarization. In the future, an in-depth investigation into the interactions of gene regulatory networks within macrophages, supported by cell-based and animal studies, may potentially unveil the underlying mechanisms that dictate the phenotypic and functional heterogeneity of Tumor-associated macrophages (TAMs). These findings open new avenues for research in NSCLC and suggest potential pathways for therapeutic interventions.

Availability of data and materials

The datasets presented in this study can be found in online repositories.

Funding

This work was supported by the National Science Foundation of China (Grant Nos. 81972313 and 81972822), the Graduate Student Scientific Research and Practice Innovation Projects in Jiangsu Province, China (Grant Nos. SJCX23_0662 and SJCX22_0672), and the Research Project of Jiangsu Cancer Hospital, China (Grant No. ZJ202207).

Declarations

Ethics approval and consent to participate.

Not applicable.

CRediT authorship contribution statement

Shaodi Wen: Writing – original draft, Visualization, Methodology, Investigation, Funding acquisition. **Renrui Zou:** Writing – original draft. **Xiaoyue Du:** Visualization. **Rongtian Pan:** Validation. **Rutao Li:** Validation. **Jingwei Xia:** Validation. **Cong Xu:** Validation. **Ruotong Wang:** Visualization. **Feng Jiang:** Writing – review & editing. **Guoren Zhou:** Writing – review & editing. **Jifeng Feng:** Writing – review & editing. **Miaolin Zhu:** Supervision, Funding acquisition. **Xin Wang:** Investigation. **Bo Shen:** Writing – review & editing, Supervision, Funding acquisition.

Declaration of competing interest

The authors declare that they have no known competing financial interests or personal relationships that could have appeared to influence the work reported in this paper.

Acknowledgements

The authors highly appreciate all the participants and their families.

Appendix A. Supplementary data

Supplementary data to this article can be found online at https://doi.org/10.1016/j.heliyon.2024.e27170.

References

[1] R.L. Siegel, K.D. Miller, H.E. Fuchs, A. Jemal, Cancer statistics, 2021, CA Cancer J Clin 71 (1) (2021) 7–33.
[2] R.L. Siegel, K.D. Miller, H.E. Fuchs, A. Jemal, Cancer statistics, CA Cancer J Clin 72 (1) (2022) 7–33.
[3] F. Bray, M. Laversanne, E. Weiderpass, I. Soerjomataram, The ever-increasing importance of cancer as a leading cause of premature death worldwide, Cancer 127 (16) (2021) 3029–3030.
[4] H. Sung, J. Ferlay, R.L. Siegel, M. Laversanne, I. Soerjomataram, A. Jemal, et al., Global cancer statistics 2020: GLOBOCAN tstimates of Incidence and mortality worldwide for 36 cancers in 185 Countries, CA Cancer J Clin 71 (3) (2021) 209–249.
[5] Surveillance, Epidemiology, and end results (SEER) Program <Katrina/Rita population Adjustment>—linked to county attributes—Total United States, 1969-2019 Counties, in: SEER*Stat Database: Incidence—SEER 18 Registries Research Data + Hurricane Katrina Impacted Louisiana Cases, National Cancer Institute, Division of Cancer Control and Population Sciences, Surveillance Research Program, 2020–2021. https://cancercontrol.cancer.gov/overview-highlights/2021/progress_srp.html.
[6] M. Wang, R.S. Herbst, C. Boshoff, Toward personalized treatment approaches for non-small-cell lung cancer, Nat Med 27 (8) (2021) 1345–1356.
[7] E.L. van Dijk, Y. Jaszczyszyn, D. Naquin, C. Thermes, The Third Revolution in sequencing technology, Trends Genet. 34 (9) (2018) 666–681.
[8] R. Stark, M. Grzelak, J. Hadfield, RNA sequencing: the teenage years, Nat. Rev. Genet. 20 (11) (2019) 631–656.
[9] P.J. Park, ChIP-seq: advantages and challenges of a maturing technology, Nat. Rev. Genet. 10 (10) (2009) 669–680.
[10] D. Jovic, X. Liang, H. Zeng, L. Lin, F. Xu, Y. Luo, Single-cell RNA sequencing technologies and applications: a brief overview, Clin. Transl. Med. 12 (3) (2022) e694.
[11] A.M. Sardoo, S. Zhang, T.N. Ferraro, T.M. Keck, Y. Chen, Decoding brain memory formation by single-cell RNA sequencing, Brief Bioinform 23 (6) (2022).
[12] H. Peng, X. Wu, S. Liu, M. He, C. Xie, R. Zhong, et al., Multiplex immunofluorescence and single-cell transcriptomic profiling reveal the spatial cell interaction networks in the non-small cell lung cancer microenvironment, Clin. Transl. Med. 13 (1) (2023) e1155.
[13] M. Fane, A.T. Weeraratna, How the ageing microenvironment influences tumour progression, Nat. Rev. Cancer 20 (2) (2020) 89–106.
[14] L. Laplane, D. Duluc, A. Bikfalvi, N. Larmonier, T. Pradeu, Beyond the tumour microenvironment, Int. J. Cancer 145 (10) (2019) 2611–2618.
[15] S. Wen, Y. Chen, C. Hu, X. Du, J. Xia, X. Wang, et al., Combination of Tertiary lymphoid structure and Neutrophil-to-Lymphocyte ratio predicts survival in patients with Hepatocellular carcinoma, Front. Immunol. 12 (2021) 788640.
[16] M. Binnewies, E.W. Roberts, K. Kersten, V. Chan, D.F. Fearon, M. Merad, et al., Understanding the tumor immune microenvironment (TIME) for effective therapy, Nat Med 24 (5) (2018) 541–550.
[17] F. Galli, J.V. Aguilera, B. Palermo, S.N. Markovic, P. Nistico, A. Signore, Relevance of immune cell and tumor microenvironment imaging in the new era of immunotherapy, J. Exp. Clin. Cancer Res. 39 (1) (2020) 89.
[18] J.M. Taube, J. Galon, L.M. Sholl, S.J. Rodig, T.R. Cottrell, N.A. Giraldo, et al., Implications of the tumor immune microenvironment for staging and therapeutics, Mod. Pathol. 31 (2) (2018) 214–234.
[19] C. Varol, A. Mildner, S. Jung, Macrophages: development and tissue specialization, Annu. Rev. Immunol. 33 (2015) 643–675.
[20] S. Dubey, S. Ghosh, D. Goswami, D. Ghatak, R. De, Immunometabolic attributes and mitochondria-associated signaling of Tumor-Associated Macrophages in tumor microenvironment modulate cancer progression, Biochem. Pharmacol. 208 (2023) 115369.
[21] S. Yan, G. Wan, Tumor-associated macrophages in immunotherapy, FEBS J. 288 (21) (2021) 6174–6186.
[22] P. Jiang, Y. Zhang, B. Ru, Y. Yang, T. Vu, R. Paul, et al., Systematic investigation of cytokine signaling activity at the tissue and single-cell levels, Nat. Methods 18 (10) (2021) 1181–1191.
[23] X. Geeraerts, E. Bolli, S.M. Fendt, J.A. Van Ginderachter, Macrophage metabolism as therapeutic target for cancer, Atherosclerosis, and Obesity, Front. Immunol. 8 (2017) 289.
[24] Y. Pan, Y. Yu, X. Wang, T. Zhang, Tumor-associated macrophages in tumor immunity, Front. Immunol. 11 (2020) 583084.
[25] M. Gerlinger, A.J. Rowan, S. Horswell, M. Math, J. Larkin, D. Endesfelder, et al., Intratumor heterogeneity and branched evolution revealed by multiregion sequencing, N. Engl. J. Med. 366 (10) (2012) 883–892.
[26] R. Evans, P. Alexander, Cooperation of immune lymphoid cells with macrophages in tumour immunity, Nature 228 (5272) (1970) 620–622.
[27] B.Z. Qian, J.W. Pollard, Macrophage diversity enhances tumor progression and metastasis, Cell 141 (1) (2010) 39–51.
[28] Q.W. Zhang, L. Liu, C.Y. Gong, H.S. Shi, Y.H. Zeng, X.Z. Wang, et al., Prognostic significance of tumor-associated macrophages in solid tumor: a meta-analysis of the literature, PLoS One 7 (12) (2012) e50946.
[29] M.D. Vesely, M.H. Kershaw, R.D. Schreiber, M.J. Smyth, Natural innate and adaptive immunity to cancer, Annu. Rev. Immunol. 29 (2011) 235–271.
[30] T. Wu, E. Hu, S. Xu, M. Chen, P. Guo, Z. Dai, et al., clusterProfiler 4.0: a universal enrichment tool for interpreting omics data, Innovation 2 (3) (2021) 100141.

[31] F. Babaie, R. Hosseinzadeh, M. Ebrazeh, N. Seyfizadeh, S. Aslani, S. Salimi, et al., The roles of ERAP1 and ERAP2 in autoimmunity and cancer immunity: new insights and perspective, Mol. Immunol. 121 (2020) 7–19.
[32] Z. Yang, H. Tian, F. Bie, J. Xu, Z. Zhou, J. Yang, et al., ERAP2 is associated with immune infiltration and predicts favorable prognosis in SqCLC, Front. Immunol. 12 (2021) 788985.
[33] H. Kazeto, S. Nomura, N. Ito, T. Ito, Y. Watanabe, H. Kajiyama, et al., Expression of adipocyte-derived leucine aminopeptidase in endometrial cancer. Association with tumor grade and CA-125, Tumour Biol 24 (4) (2003) 203–208.
[34] A.M. Mehta, E.S. Jordanova, T. van Wezel, H.W. Uh, W.E. Corver, K.M. Kwappenberg, et al., Genetic variation of antigen processing machinery components and association with cervical carcinoma, Genes Chromosomes Cancer 46 (6) (2007) 577–586.
[35] J. Klunk, T.P. Vilgalys, C.E. Demeure, X. Cheng, M. Shiratori, J. Madej, et al., Evolution of immune genes is associated with the Black Death, Nature 611 (7935) (2022) 312–319.
[36] P. Binarova, J. Tuszynski, Tubulin: structure, functions and roles in disease, Cells 8 (10) (2019).
[37] M.Z. Nassef, S. Kopp, M. Wehland, D. Melnik, J. Sahana, M. Kruger, et al., Real Microgravity influences the Cytoskeleton and Focal Adhesions in human Breast cancer cells, Int. J. Mol. Sci. 20 (13) (2019).
[38] B. Kim, M. Jung, K.C. Moon, D. Han, K. Kim, H. Kim, et al., Quantitative proteomics identifies TUBB6 as a biomarker of muscle-invasion and poor prognosis in bladder cancer, Int. J. Cancer 152 (2) (2023) 320–330.
[39] T.R. Pisanic, L.M. Cope, S.F. Lin, T.T. Yen, P. Athamanolap, R. Asaka, et al., analysis of Ovarian cancers identifies tumor-specific Alterations Readily detectable in early Precursor Lesions, Clin. Cancer Res. 24 (24) (2018) 6536–6547.
[40] X. Lin, T. Zhou, S. Hu, L. Yang, Z. Yang, H. Pang, et al., Prognostic significance of pyroptosis-related factors in lung adenocarcinoma, J. Thorac. Dis. 14 (3) (2022) 654–667.
[41] C. Xu, L. Fan, Y. Lin, W. Shen, Y. Qi, Y. Zhang, et al., Fusobacterium nucleatum promotes colorectal cancer metastasis through miR-1322/CCL20 axis and M2 polarization, Gut Microb. 13 (1) (2021) 1980347.
[42] H.T. Meitei, N. Jadhav, G. Lal, CCR6-CCL20 axis as a therapeutic target for autoimmune diseases, Autoimmun. Rev. 20 (7) (2021) 102846.
[43] B. Nandi, C. Pai, Q. Huang, R.H. Prabhala, N.C. Munshi, J.S. Gold, CCR6, the sole receptor for the chemokine CCL20, promotes spontaneous intestinal tumorigenesis, PLoS One 9 (5) (2014) e97566.
[44] P. Scapini, C. Laudanna, C. Pinardi, P. Allavena, A. Mantovani, S. Sozzani, et al., Neutrophils produce biologically active macrophage inflammatory protein-3alpha (MIP-3alpha)/CCL20 and MIP-3beta/CCL19, Eur. J. Immunol. 31 (7) (2001) 1981–1988.
[45] T. Yamazaki, X.O. Yang, Y. Chung, A. Fukunaga, R. Nurieva, B. Pappu, et al., CCR6 regulates the migration of inflammatory and regulatory T cells, J. Immunol. 181 (12) (2008) 8391–8401.
[46] X.P. Zhang, Z.J. Hu, A.H. Meng, G.C. Duan, Q.T. Zhao, J. Yang, Role of CCL20/CCR6 and the ERK signaling pathway in lung adenocarcinoma, Oncol. Lett. 14 (6) (2017) 8183–8189.
[47] L. Sanchez-Caballero, B. Ruzzenente, L. Bianchi, Z. Assouline, G. Barcia, M.D. Metodiev, et al., Mutations in complex I assembly factor TMEM126B result in muscle Weakness and Isolated complex I deficiency, Am. J. Hum. Genet. 99 (1) (2016) 208–216.
[48] C.L. Alston, A.G. Compton, L.E. Formosa, V. Strecker, M. Olahova, T.B. Haack, et al., Biallelic mutations in TMEM126B cause Severe complex I deficiency with a variable clinical phenotype, Am. J. Hum. Genet. 99 (1) (2016) 217–227.
[49] D.C. Fuhrmann, I. Wittig, S. Drose, T. Schmid, N. Dehne, B. Brune, Degradation of the mitochondrial complex I assembly factor TMEM126B under chronic hypoxia, Cell. Mol. Life Sci. 75 (16) (2018) 3051–3067.
[50] D.C. Fuhrmann, I. Wittig, B. Brune, TMEM126B deficiency reduces mitochondrial SDH oxidation by LPS, attenuating HIF-1alpha stabilization and IL-1beta expression, Redox Biol. 20 (2019) 204–216.